# CHAPTER VI

## COMPUTER SIMULATIONS FOR TYPE I SUPERCONDUCTORS

### Introduction

It is well known that the Ginzburg-Landau theory provides us with an important and useful tool for studying the basic phenomenology of superconductivity. Since the discovery of high-temperature superconductors, the Ginzburg-Landau theory has played an especially useful role for understanding and analysis. Some physical properties of those superconductors are not well understood, because there is at the present time no clear understanding of the microscopic mechanism of high-$T_c$ superconductors.

There appear to have been few numerical attempts to solve the Ginzburg-Landau equations. Those commonly referenced are by Abrikosov (1957), Kleiner (1964), Brandt (1972), Doria (1990), Wang (1991) , Du (1992) and Garner (1990).

In this chapter we numerically minimize the total Gibbs free energy of the sample. At that minimum energy state, the behavior of the order parameter $\Psi$ and supervelocity $\mathbf{Q}$ in the superconducting materials is revealed.

Lattice Equation

We start with the Gibbs free energy density (eq. 4.5) as follows:

$$g = -\Psi^2 + 0.5\Psi^4 + (\nabla\Psi)^2 + \mathbf{Q}^2\Psi^2 + \kappa^2(\nabla\times\mathbf{Q} - \mathbf{H})^2 \qquad (6.1)$$

The basic idea of this thesis is very straightforward. We need not minimize the Gibbs free energy analytically with respect to $\Psi$ or to $\mathbf{Q}$, which leads to the Ginzburg-Landau equations. Instead, we will minimize eq.(6.1) directly by numerical methods.

For one dimension, we assume that the (constant) external magnetic field **H** is in the $\hat{\mathbf{z}}$ direction, as shown in fig. 6.1. The internal magnetic field **h** is in the same direction as **H**.

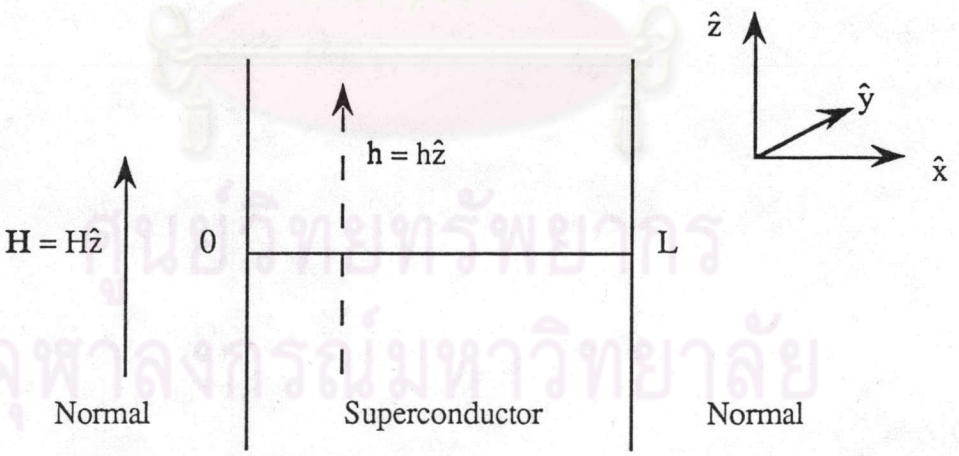


Fig. 6.1 Diagram of a superconductor of width L. The applied magnetic field **H** is lies along the $\hat{\mathbf{z}}$ direction.

If we choose $\mathbf{Q} = Q(x)\,\hat{\mathbf{y}}$, and use

$$\mathbf{h} = \nabla\times\mathbf{Q} = \begin{vmatrix} \hat{\mathbf{x}} & \hat{\mathbf{y}} & \hat{\mathbf{z}} \\ \frac{\partial}{\partial x} & \frac{\partial}{\partial y} & \frac{\partial}{\partial z} \\ 0 & Q(x) & 0 \end{vmatrix}$$

$$= \frac{dQ(x)}{dx}\hat{\mathbf{z}} = h(x)\,\hat{\mathbf{z}} \qquad (6.2)$$

eq.(6.1) becomes

$$g = -\Psi^2 + 0.5\Psi^4 + \left(\frac{d\Psi}{dx}\right)^2 + Q(x)^2\Psi^2 + \kappa^2\left(\frac{dQ(x)}{dx} - H\right)^2 \qquad (6.3)$$

The total Gibbs free energy is

$$G = \frac{1}{V}\int d^3x\left[-\Psi^2 + 0.5\Psi^4 + (\nabla\Psi)^2 + \mathbf{Q}^2\Psi^2 + \kappa^2(\nabla\times\mathbf{Q} - \mathbf{H})^2\right] \qquad (6.4)$$

and from eq. (6.3) we have

$$G = \frac{1}{L}\int dx\left[-\Psi^2 + 0.5\Psi^4 + \left(\frac{d\Psi}{dx}\right)^2 + Q^2(x)\Psi^2 + \kappa^2\left(\frac{dQ(x)}{dx} - H\right)^2\right] \qquad (6.5)$$

ศูนย์วิทยทรัพยากร
จุฬาลงกรณ์มหาวิทยาลัย

where V is the volume and L is the length of the superconducting material in the x direction.

Discretizing eq(6.5) , we get

$$G = \frac{1}{N}\sum_{i=1}^{N+1}\left[-\Psi_i^2 + 0.5\Psi_i^4 + \left(\frac{\Psi_{i+1} - \Psi_{i-1}}{2\Delta x}\right)^2 + Q_i^2\Psi_i^2 + \kappa^2\left(\frac{Q_{i+1} - Q_{i-1}}{2\Delta x} - H\right)^2\right] \tag{6.6}$$

where the superconducting sample was divided into N strips along the $\hat{x}$ direction, and $\Delta x$ is an infinitesimal length between point i and point i+1, as shown in fig 6.2:

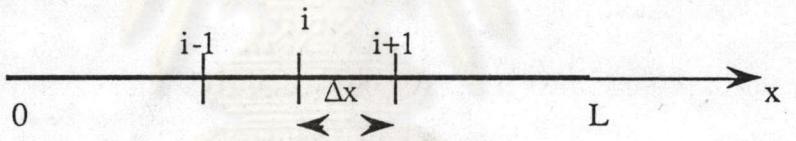


Fig. 6.2 Discretization of a superconducting sample in one dimension.

Therefore, we need to solve for $\Psi$ and Q as functions only of x. We will see that on each lattice point the order parameter has the value $\Psi_i$ and the supervelocity has value $Q_i$, which are variables in this program.

Numerical Techniques

Since the general form of eq.(6.6) can be written as

$$G = G(\Psi_1 \ldots, \Psi_{N+1}, Q_1 \ldots, Q_{N+1}) \tag{6.7}$$

we have 2(N+1) variables . The boundary condition was chosen as

$$\Psi(0) = \Psi(L) = 0 \qquad (6.8)$$

The principle of this program is that we first set all the values of the order parameter $\Psi$ equal to 1.0 , except at the boundary where we keep it equal to 0.0 forever (assuming a normal metal is at each end). For the supervelocity we start with 0.0 at every point. After that the free energy was calculated.Then the values of $\Psi$ and Q were changed randomly using the subroutine URAND (the source code of this program is listed in appendix A). After that the free energy calculation was done again and again, and the free energy became lower and lower. Only configurational changes leading to a lower free energy were accepted. When the free energy reaches a minimum, the program will stop. As a result we find the desired values of the order parameter and supervelocity at each point. The internal magnetic field was calculated from the following relation :

$$h_i = \frac{Q_{i+1} - Q_{i-1}}{2\Delta x} \qquad (6.9)$$

ศูนย์วิทยทรัพยากร
จุฬาลงกรณ์มหาวิทยาลัย

Results and Conclusion

The simulation requires the specification of N, L, $\kappa$, and H. N is the number of strips. L is the length of superconducting sample in units of the coherence length ($\xi$). In addition, $\kappa$ is the Ginzburg-Landau parameter, and H is the external magnetic field. Recall that $H_c = 1/\kappa\sqrt{2}$ is the critical magnetic field in our units.

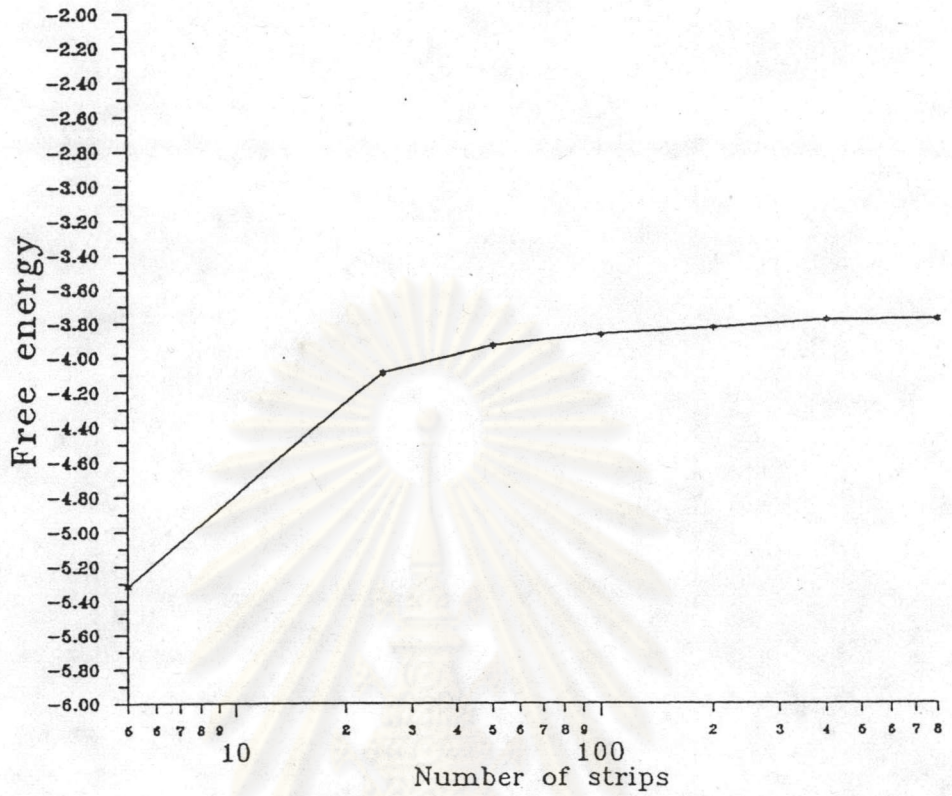


Fig 6.3 The free energy vs. the number of strips.

The first problem is how to choose the appropriate number of strips for our simulation. We fixed $\kappa = 0.5$, $H = 1.0$, and $L = 20\xi$, and varied the number of strips from 5, 25, 50, 100, 200, 400, 800. The result of each simulation is shown in fig 6.3. From fig 6.3 we see that when more than 100 strips were used, the free energy was quite the same , so only 100 strips are sufficient for our simulation.

No Magnetic Field

For the case of no external magnetic field, we chose H = 0, L = 20.0 $\xi$, and $\kappa$ = 0.5. The result is shown in fig. 6.4.

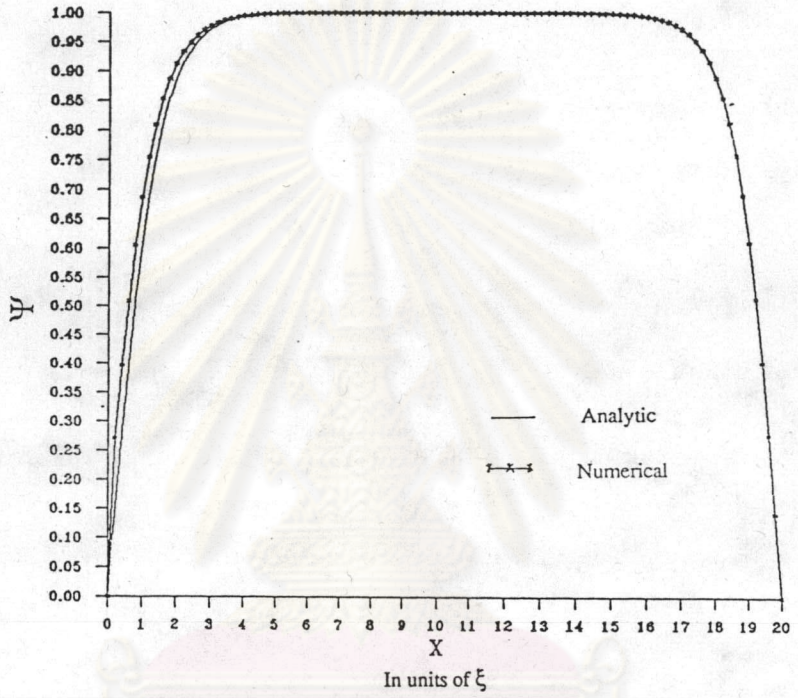


Fig.6.4 Numerical and analytical solution for the order parameter vs. x for the case of no external magnetic field, where L = 20$\xi$, $\kappa$ = 0.5.

The approximate analytical solution for this case is

$$\Psi = \tanh\left(\frac{x}{\sqrt{2}}\right)\tanh\left(\frac{L-x}{\sqrt{2}}\right) \qquad (6.10)$$

(compare chapter II with one boundary), we can derive an approximate analytical solution as following. In the thick sample limit (L >> $\xi$), the first Ginzburg-Landau equation is satisfied by eq.(6.10), as follows:

$$\frac{d^2\Psi}{dx^2} + \Psi - \Psi^3 = 0 \qquad (6.11)$$

$$\frac{d^2\Psi}{dx^2} + \Psi = \Psi\left[1 - \operatorname{sech}^2\left(\frac{x}{\sqrt{2}}\right) - \operatorname{sech}^2\left(\frac{L-x}{\sqrt{2}}\right)\right] - \operatorname{sech}^2\left(\frac{x}{\sqrt{2}}\right)\operatorname{sech}^2\left(\frac{L-x}{\sqrt{2}}\right) \qquad (6.12)$$

$$\Psi^3 = \Psi\left[1 - \operatorname{sech}^2\left(\frac{x}{\sqrt{2}}\right) - \operatorname{sech}^2\left(\frac{L-x}{\sqrt{2}}\right) + \operatorname{sech}^2\left(\frac{x}{\sqrt{2}}\right)\operatorname{sech}^2\left(\frac{L-x}{\sqrt{2}}\right)\right] \qquad (6.13)$$

so that eq.(6.10) is an exact solution only if $L \to \infty$, when eqs.(6.12) and (6.13) will be equal, since $\operatorname{sech}^2\{x/\sqrt{2}\}\operatorname{sech}^2\{(L-x)/\sqrt{2}\} \to 0$. This approximate analytic solution is also shown in fig. 6.4.

When the condition $L >> \xi$ is <u>not</u> satisfied, i.e. the sample is thin, we can no longer solve eq.(6.10) analytically. However, the numerical method can easily be applied in this regime (fig. 6.5). Thus we can use the numerical approach in a situation which is inaccessible analytically.

Unfortunately, this thin-sample solution is not very useful for actual superconductors. The reason is that the Ginzburg-Landau equations have a defect : they do not give the correct boundary condition for the order parameter $\Psi$. Physically, $d\Psi/dx$ should be zero at a boundary (Lifshitz and Pitaevskii, 1980). However, the Ginzburg-Landau equations yield solutions where $d\Psi/dx \neq 0$ at the boundaries (see figs. 6.4 and 6.5). This defect is not important for thick samples. However, for thin

samples it can be important, and in that case the Ginzburg-Landau theory is not appropriate.

Applied Magnetic Field Case

When there is an external magnetic field, some of the magnetic field intensity can penetrate a short distance into the sample, even when the external magnetic field is lower than the critical magnetic field $H_c$ and the sample is in the Meissner state. A schematic indication is shown in fig 6.6.

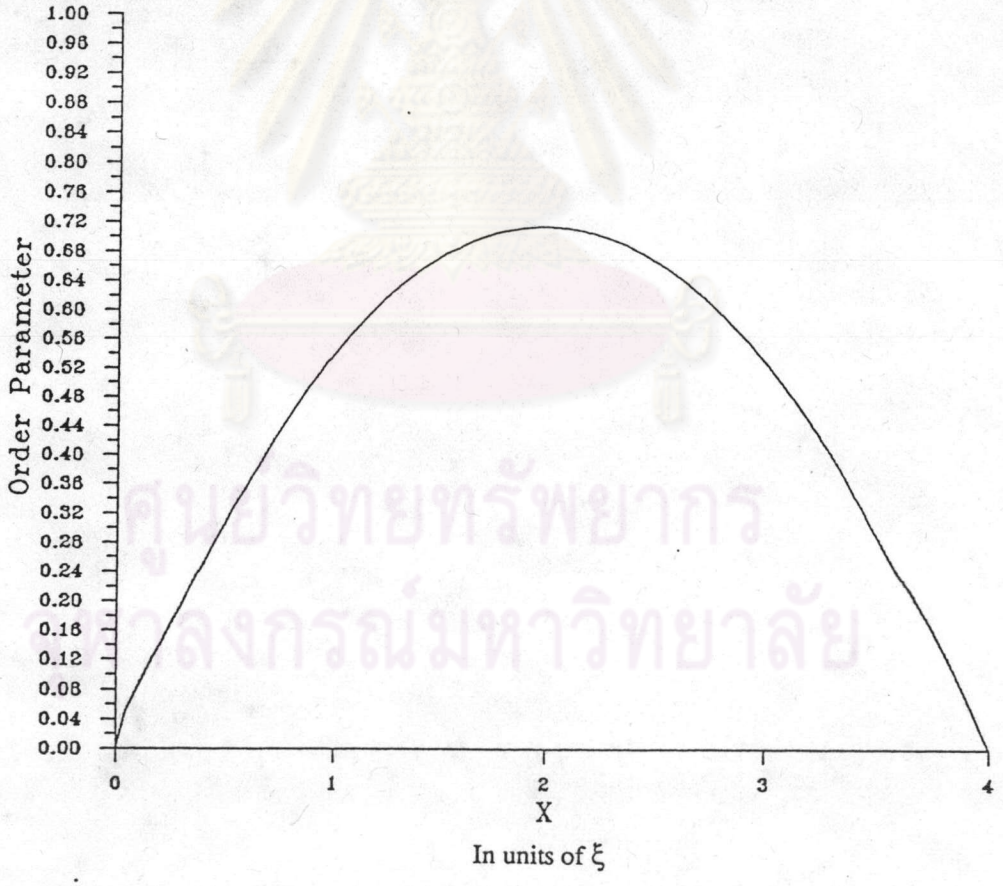


Fig. 6.5 The order parameter ($\Psi$) vs. x for a thin sample,where $H = 0.0$, $L = 4\xi$, $\kappa = 0.5$

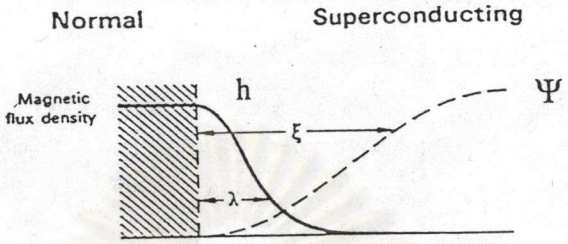


Fig. 6.6 Order parameter and internal magnetic field of a superconductor with one boundary (Rose-Innes and Rhoderick, 1978).

Our simulation can produce this behavior very well as shown in fig 6.7. We chose an applied magnetic field H = 1.0, the Ginzburg-Landau parameter $\kappa = 0.5$, and $L = 20\xi$.

Recall that the supervelocity Q , which can be interpreted as the velocity of superelectrons, characterizes the supercurrent, which is proportional to $Q\Psi^2$, where the quantity $\Psi^2$ represents the density of superelectrons. In fig 6.8 we show graphs of the internal magnetic field for many values of $\kappa$, when the external magnetic field H was fixed at $H = 1.0$ and $L = 20\xi$. We will see that the penetration of internal magnetic field depends on the penetration depth $\lambda$ (remember that $\kappa = \lambda/\xi$, and $\xi = 1$ in these units).

For the next simulation we vary the external magnetic field, keeping the Ginzburg-Landau parameter $\kappa = 0.5$, and $L = 20\xi$ fixed. Since the critical magnetic field $H_c = 1/\kappa\sqrt{2}$ in our units, from figs. 6.9, 6.10 and 6.11 we can see that when the

external magnetic field H is less than the critical value $H_c$ , the magnetic field can penetrate through the sample only over a range approximately equal to the value of κ, after which the Meissner effect is complete. When the external magnetic field is equal to or greater than $H_c$ the external magnetic field can penetrate completely through the superconductor, with an amount equal to the external value, and the superconductivity is destroyed completely. The sample is now in a normal state. In figs. 6.12 and 6.13 we show the precision of this program in predicting the breakdown of superconductivity at the critical field, $H_c = 1.414$.

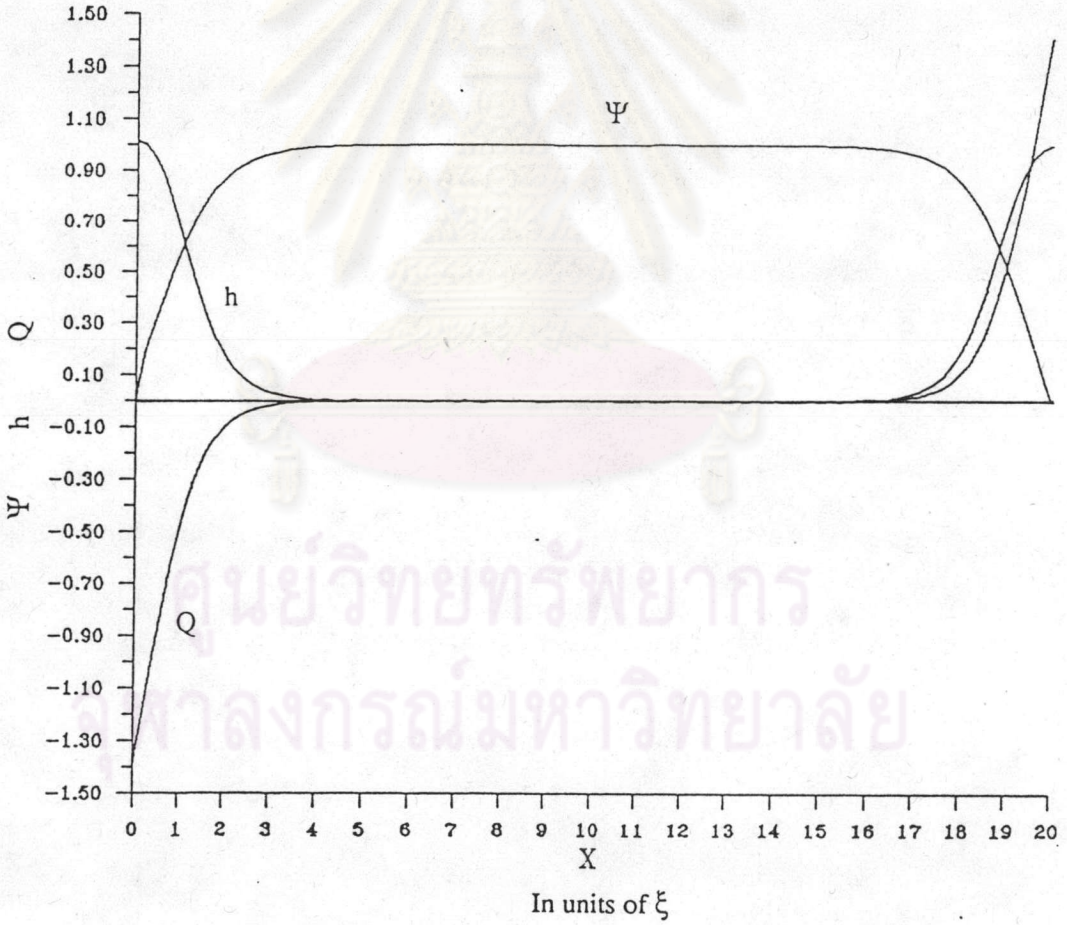


Fig. 6.7 Numerical results for the order parameter (Ψ), internal magnetic field (h), and supervelocity(Q), where H = 1.0, κ = 0.5, L = 20ξ.

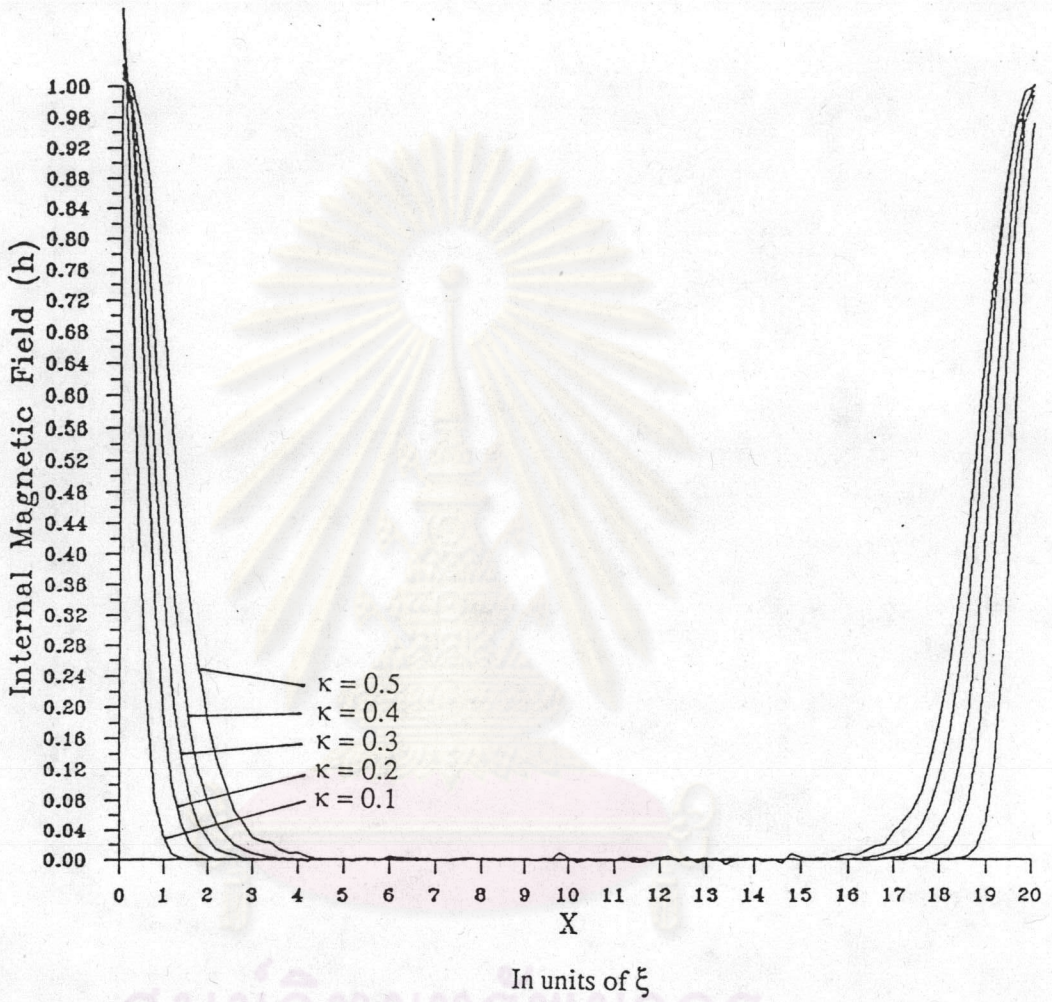


Fig. 6.8 The internal magnetic field h vs. x for various values of κ.

ศูนย์วิทยทรัพยากร
จุฬาลงกรณ์มหาวิทยาลัย

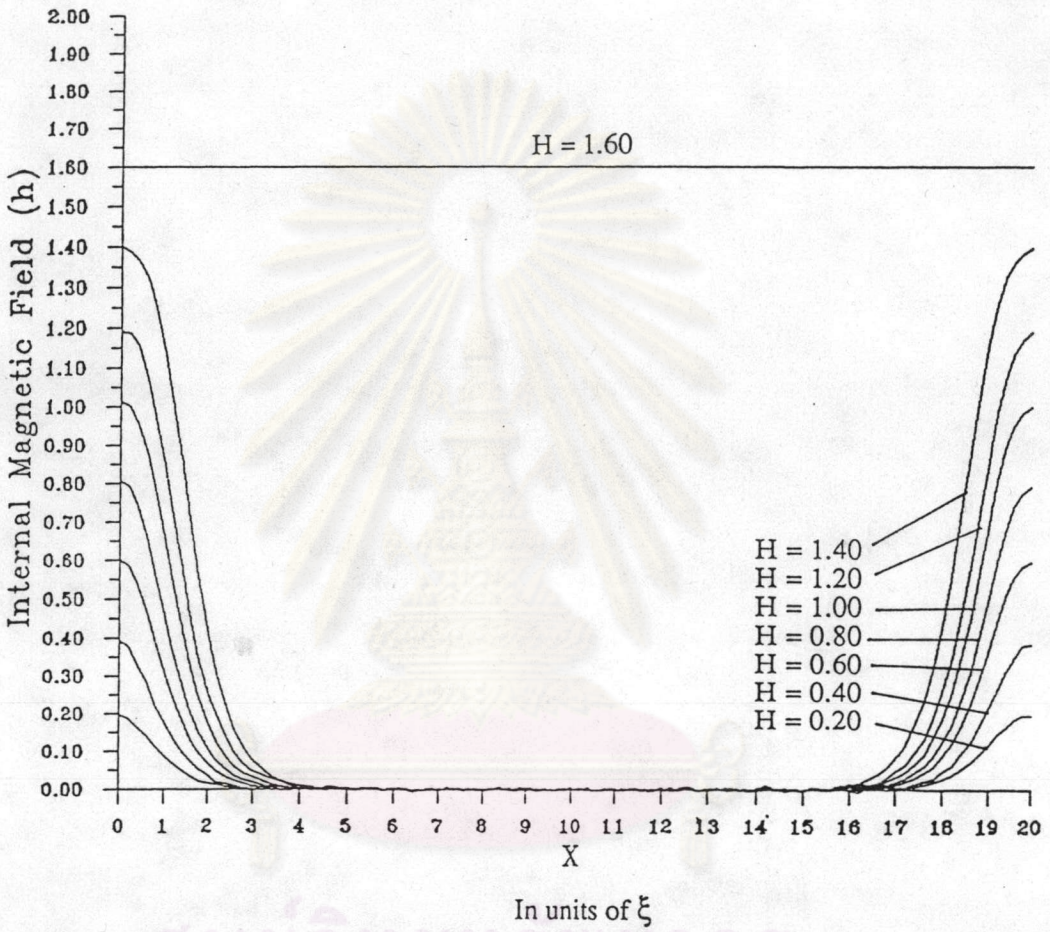


Fig. 6.9 The internal magnetic field vs. x for various values of the external magnetic field (H) values. The critical magnetic field $H_c = 1.414$, $\kappa = 0.5$.

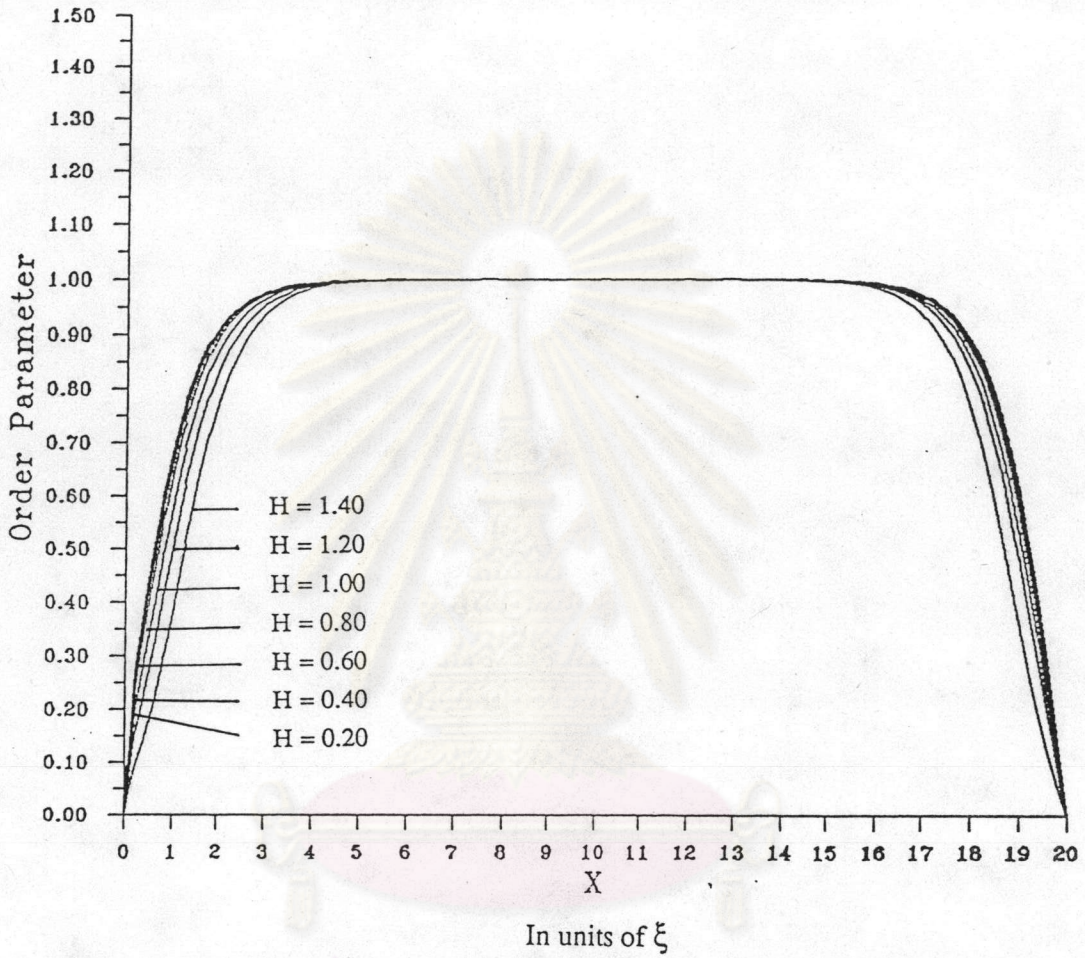


Fig. 6.10 The order parameter (Ψ) vs. x for various H values.

ศูนย์วิทยทรัพยากร
จุฬาลงกรณ์มหาวิทยาลัย

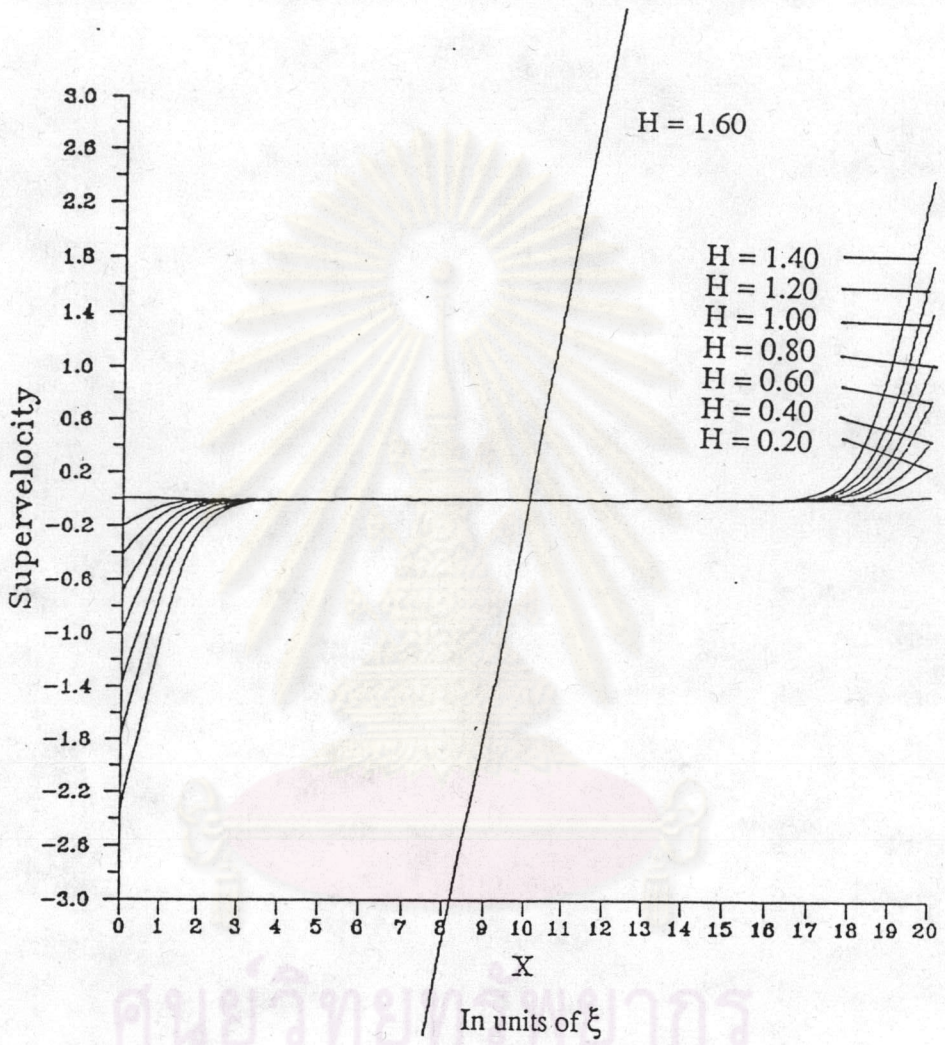


Fig. 6.11 The supervelocity (Q ) vs. x for various H values.

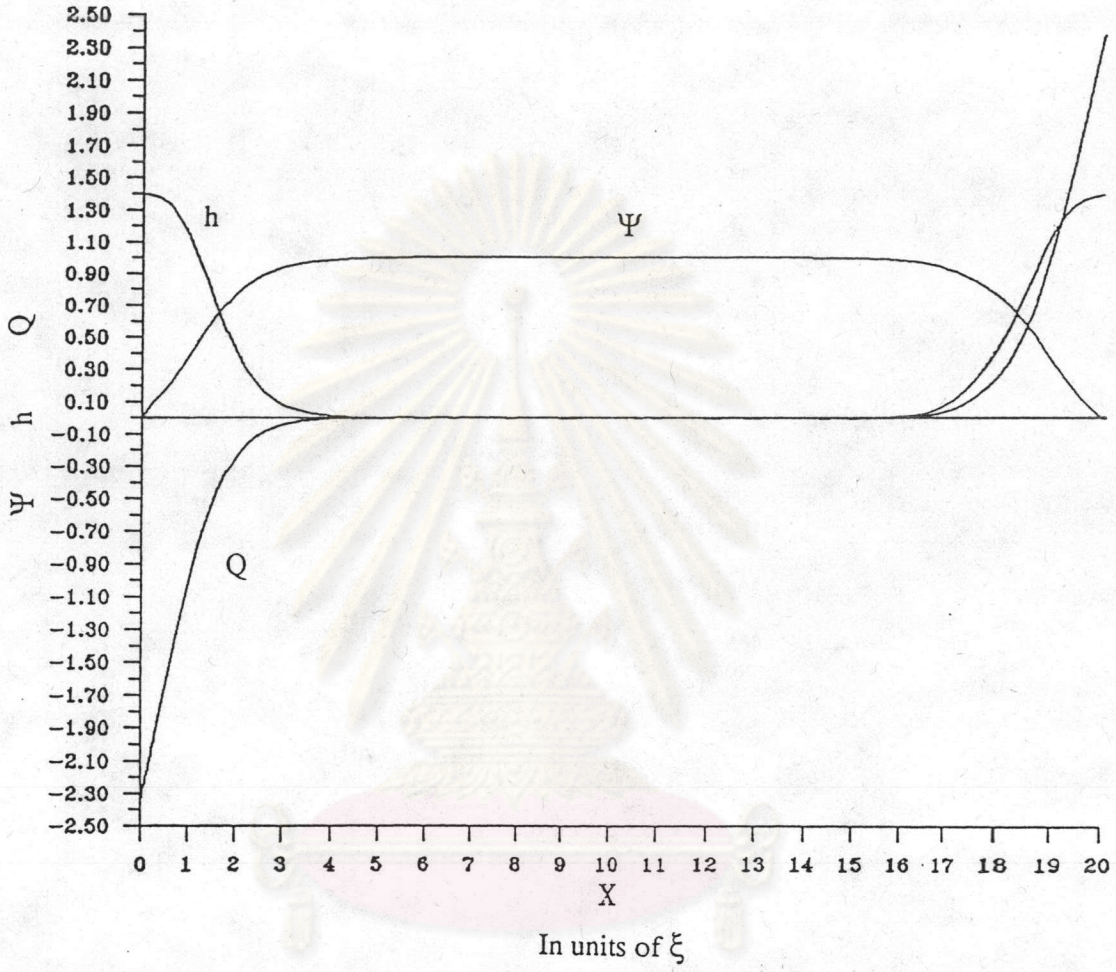


Fig. 6.12 The order parameter (Ψ), internal magnetic field (h), and supervelocity (Q)vs. x for H = 1.40.

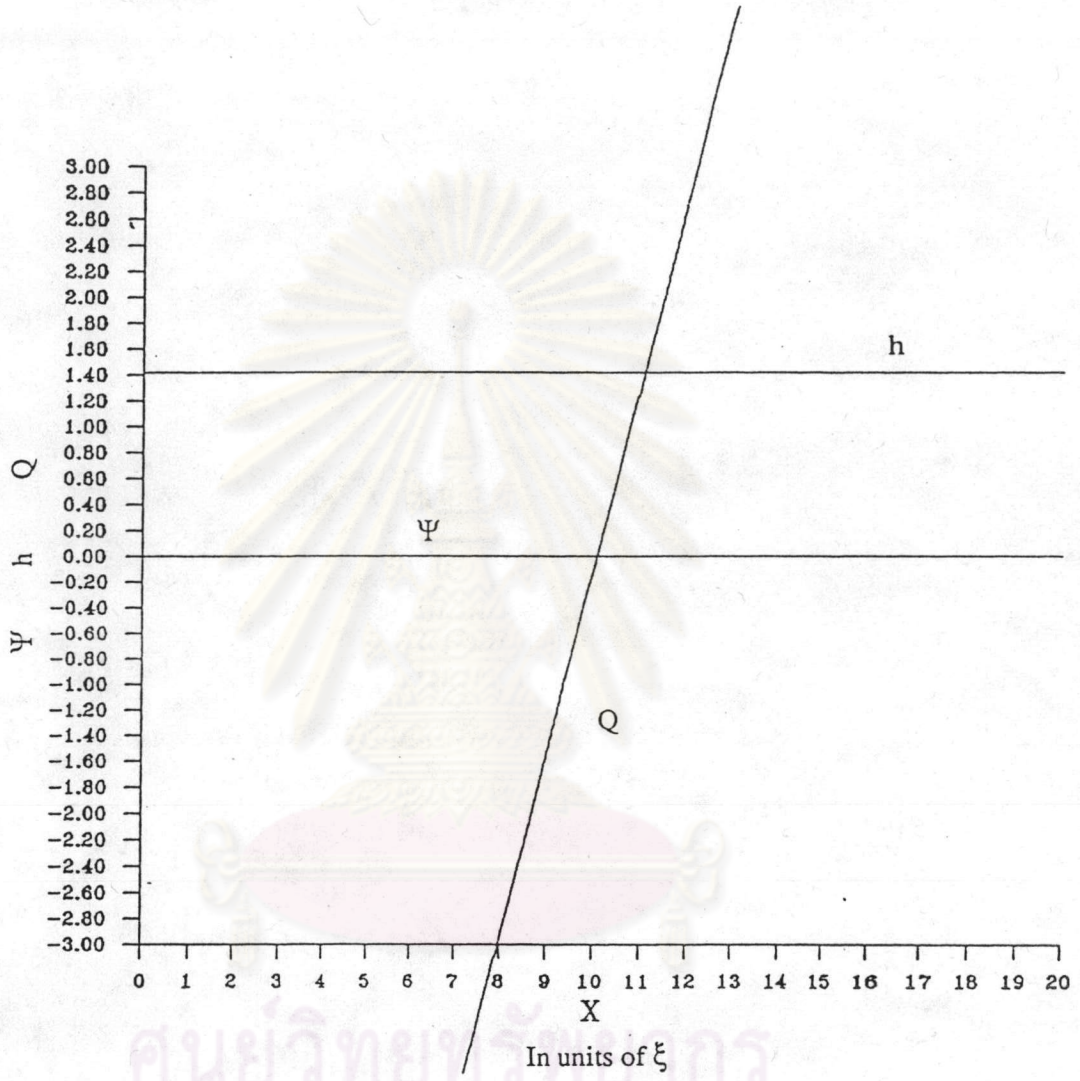


Fig. 6.13 The order parameter (Ψ), internal magnetic field (h), and supervelocity (Q)vs. x for H = 1.42.

($H_c$ = 1.414 in these units)